Electronic Supplementary Material (ESI) for Metallomics

Supplemental material

Co(II)-detection does not follow $K_{Co(II)}$ gradient: Channelling in Co(II)-sensing

Carl J. Patterson[1], Rafael Pernil[1], Samantha J. Dainty,[1] Buddhapriya Chakrabarti[3], Clare E. Henry[2], Victoria A. Money[2], Andrew W. Foster[1,4] and Nigel J. Robinson[1,2]

Biophysical Sciences Institute, Durham University, DH1 3LE, UK and Departments/Schools of [1]Biological and Biomedical Sciences, [2]Chemistry and [3]Mathematics and [4]ICAMB, Newcastle University, UK.

Email Correspondence*:* nigel.robinson@durham.ac.uk

TABLE OF CONTENTS

Table S1. Primers/oligonucletides used in this work

Primer	No.	Use	Sequence 5'-3'
CoaR-S167A-F	1	CoaR SDM[a]	CCAGAAGCCTTCCAGGAAGCCCTCAAACACCTGCTAC
CoaR-S167A-R	2	CoaR SDM[a]	GTAGCAGGTGTTTGAGGGCTTCCTGGAAGGCTTCTGG
CoaR-S290A-F	3	CoaR SDM	GCGATCGGCTATGCCCCTGCTGTTTTACTCACTGCC
CoaR-S290A-R	4	CoaR SDM	GGCAGTGAGTAAAACAGCAGGGGCATAGCCGATCGC
CoaR-H266A-F	5	CoaR SDM	CGAGCAAGCTTTTTGGGCCCATGACCATTGGCAACAGC
CoaR-H266A-R	6	CoaR SDM	GCTGTTGCCAATGGTCATGGGCCCAAAAAGCTTGCTCG
CoaR-D250A-F	7	CoaR SDM	GGTTAAAACGCTGATTGCCGACCCTCACATCACAGGG
CoaR-D250A-R	8	CoaR SDM	CCCTGTGATGTGAGGGTCGGCAATCAGCGTTTTAACC
CoaR-Y287F-F	9	CoaR SDM[a]	GTGTGCTGGCAATCGGCTTTGCCCCTTCTGTTTTAC
CoaR-Y287F-R	10	CoaR SDM[a]	GTAAAACAGAAGGGGCAAAGCCGATTGCCAGCACAC
CoaR-Y287E-F	11	CoaR SDM	GTGTGCTGGCAATCGGCGAGGCCCCTTCTGTTTTAC
CoaR-Y287E-R	12	CoaR SDM	GTAAAACAGAAGGGGCCTCGCCGATTGCCAGCACAC
CoaR-Q188A-F	13	CoaR SDM	CCATTCACTTACTACATGCATTAGTGCTGGCCTGTGG
CoaR-Q188A-R	14	CoaR SDM	CCACAGGCCAGCACTAATGCATGTAGTAAGTGAATGG
CoaR-C121G-F	15	CoaR SDM[a]	GGACGCGACCAGAGTGGCCAGATTACCCAAG
CoaR-C121G-R	16	CoaR SDM[a]	CTTGGGTAATCTGGCCACTCTGGTCGCGTCC
CoaR-C363G-F	17	CoaR SDM[a]	GCAAAGCCAGATGGCCACTGCTATCTC
CoaR-C363G-R	18	CoaR SDM[a]	GAGATAGCAGTGGCCATCTGGCTTTGC
ZiaR-H116R-F	19	ZiaR SDM	AGCTTGGCGCATAATCGCGTGATGAATTTGTATCGGG
ZiaR-H116R-R	20	ZiaR SDM	CCCGATACAAATTCATCACGCGATTATGCGCCAAGCT
ZiaR-C71S/C73S-F	21	ZiaR SDM	CGGCATTGGCCCGCCAAGAACTCAGTGTCAGTGATTTAG CAGCGGCG
ZiaR-C71S/C73S-R	22	ZiaR SDM	CGCCGCTGCTAAATCACTGACACTGAGTTCTTGGCGGGC CAATGCCG
RTCoaT-F	23	RT-PCR	GTGTGATTCGTTTGGTTCAGC
RTCoaT-R	24	RT-PCR	TTTGCAGAAGTTTGTCGGTGG
coa-O/P DNA primer 1	25	Fluorescence Anisotropy	[b]HEX-CAAAACCTTGACATTGACACTAATGTTAAGGTTTAG
coa-O/P DNA primer 2	26	Fluorescence Anisotropy	CTAAACCTTAACATTAGTGTCAATGTCAAGGTTTTG

[a]Primers used for mutagenesis of *coaR* in both pET29a and pET3a*coa* constructs. [b] Hex = hexachlorofluoroscein. SDM; Site-Directed Mutagenesis

Table S2. Determination of InrS $K_{Co(II)}$ affinity by competition with Fura-2

[InrS][a] (μM)	10.3	10.3	10.3
[fura2] (μM)	5.14	5.14	5.14
[Co(II)] (μM)	2.55	2.55	2.55
$F_{510\ nm}$[b]	310.37	319.39	319.58
m[c]	-104.96	-104.96	-104.96
c[c]	498.26	498.26	498.26
[Co(II)-InrS][b] (μM)	0.76	0.85	0.85
[Co(II)-fura2][b] (μM)	1.79	1.7	1.7
$K_{Co(II)}$ (M)	8.92×10^{-9}	7.09×10^{-9}	7.06×10^{-9}
Average $K_{Co(II)}$ (M)	$7.69(\pm 1.1^{d}) \times 10^{-9}$		

[a]monomer concentration, the concentration of a single tightest site is taken to be a quarter of this value as the protein exists as a tetramer. [b] equilibrium values. [c] gradient (m) and intercept (c) of Fura-2 cobalt titration standard curve produced concurrently with competition experiment. [d] standard deviation.

InrS $K_{Co(II)}$ values were calculated assuming a single tight competing site per tetramer. There is evidence for a secondary, spectrally silent Co(II) binding site on InrS (Fig. S3),[1] which may have an affinity similar to the spectrally active site. Recalculating assuming the presence of two equally competitive sites per tetramer (each with of substantially tighter $K_{Co(II)}$ than the remaining sites on the tetramer) gives a $K_{Co(II)}$ = $1.90(\pm 0.23) \times 10^{-8}$ M.

$K_{Co(II)}$ values were determined using equation 1 as described previously;[1]

$$K_D K_A' = \frac{([P]_{total} / [MP]) - 1}{([L]_{total} / [ML]) - 1} \quad (1)$$

Where $[P]_{total}$ is the concentration of tightest competing site for each protein, [L] = [Fura-2] and [ML] = [Co(II)-Fura-2] (at equilibrium). [ML] is calculated from y = mx + c describing the calibration curve produced via quenching of Fura-2 fluorescence on titration with Co(II) in figure 2; where y is the F_{510nm} intensity at equilibrium in a solution of protein, Fura-2 and Co(II), c is the y-intercept representing the F_{510nm} intensity (apo-Fura-2), m is the gradient of the calibration curve and x is [Co(II)-Fura-2]. Because total [M] in the reaction is known, [Co(II)-protein], (i.e. [MP]), can be calculated when [Co(II)-Fura-2] has been determined. K_A' is the association constant of Fura-2 with Co(II) at pH 7.8 (1.42×10^8 M^{-1}). This value was determined by competition with NTA (see supplementary Fig. S4).

Table S3. Determination of ZiaR $K_{Co(II)}$ by competition with Fura-2

[ZiaR][a] (μM)	5.2	5.2	5.2
[fura2] (μM)	4.5	4.5	4.5
[Co(II)] (μM)	2.55	2.55	2.55
$F_{510\,nm}$[b]	394.31	397.18	386.03
m[c]	-109.64	-109.64	-109.64
c[c]	478.05	478.05	478.05
[Co(II)-ZiaR][b] (μM)	1.79	1.82	1.71
[Co(II)-fura2][b] (μM)	0.76	0.73	0.84
$K_{Co(II)}$ (M)	6.51×10^{-10}	5.96×10^{-10}	8.34×10^{-10}
Average $K_{Co(II)}$ (M)	$6.94(\pm 1.3^{d}) \times 10^{-10}$		

[a] monomer concentration, the concentration of tightest site is taken to be half this value as the protein exists as a dimer. [b] equilibrium values. [c] gradient (m) and intercept (c) of Fura-2 cobalt titration standard curve produced concurrently with competition experiment. [d] standard deviation.

Table S4. Determination of Zn_1Zur $K_{Co(II)}$ by competition with Fura-2

[Zur][a] (μM)	5.1	5.1	5.1
[fura2] (μM)	4.92	4.92	4.92
[Co(II)] (μM)	2.55	2.55	2.55
$F_{510\,nm}$[b]	417.05	419.49	418.7
m[c]	-113.2	-113.2	-113.2
c[c]	497.88	497.88	497.88
[Co(II)-Zur][b] (μM)	1.84	1.86	1.85
[Co(II)-fura2][b] (μM)	0.71	0.69	0.7
$K_{Co(II)}$ (M)	$4.62x10^{-10}$	$4.67x10^{-10}$	$4.38x10^{-10}$
Average $K_{Co(II)}$ (M)	$4.56(\pm 0.16$[d]$)x10^{-10}$		

[a] monomer concentration, the concentration of tightest site is taken to be half this value as the protein exists as a dimer. [b] equilibrium values. [c] gradient (m) and intercept (c) of Fura-2 cobalt titration standard curve produced concurrently with competition experiment. [d] standard deviation.

Table S5. Summary of candidate CoaR residues binding a putative tetrapyrrole to CoaR.

Structurally conserved residue in CoaR	Results of structural modelling	Role of structurally proximal CobH residue
Ser167	CoaR Ser167 overlays in structure with Ser17 in CobH	H-bond from side chain to HBA and His43
Gln188	CoaR Gln188 close in structure to Arg40 in CobH.	H-bond from side chain and backbone N to HBA (Ala44 H-bonds to the same HBA COOH as the backbone N of Arg40)
Ser290	CoaR Ser290 overlays with Thr140 in CobH.	H-bond from side chain to HBA. Thr140 H-bonds to the same –COOH group on HBA as Thr115 in CobH
Tyr287	CoaR Tyr287 approaches the modelled HBA from opposite side to that of ligand Tyr14 in CobH	H-bond from side chain to HBA
His266	CoaR His266 close in structure to Arg116 in CobH	H-bond from side chain to HBA
His267	CoaR His267 is close in structure to Ser117 in CobH	H-bond from side chain to HBA
Asp250	CoaR Asp250 overlays Arg101 in CobH	H-bond from side chain to HBA
Trp265	CoaR Trp265 overlays T115 in CobH	H-bond from side chain to HBA (same COOH group as Thr140)
Leu191	Leu191 in CoaR overlays His43 in CobH	H-bond from side chain to Ser17
Gly342	Gly342 in CoaR close to Ser195 in CobH	H-bond from side chain (via a water molecule) to HBA
Ala192	Ala192 in CoaR overlays Ala44 in CobH	H-bond from backbone N to HBA (same COOH group as Arg40)

The residues identified as candidate tetrapyrrole ligands in CoaR based on comparison to the CobH-HBA co-crystal structure.[2] Residues Trp265, Leu191, Gly342 in CoaR closely overlapped in space with tetrapyrrole ligands in CobH but do not conserve hydrogen bonding side chains and so were not mutated. CoaR Ala192 overlays Ala44 in CobH, however, Ala44 binds to HBA via a backbone hydrogen bond and hence it was not mutated.

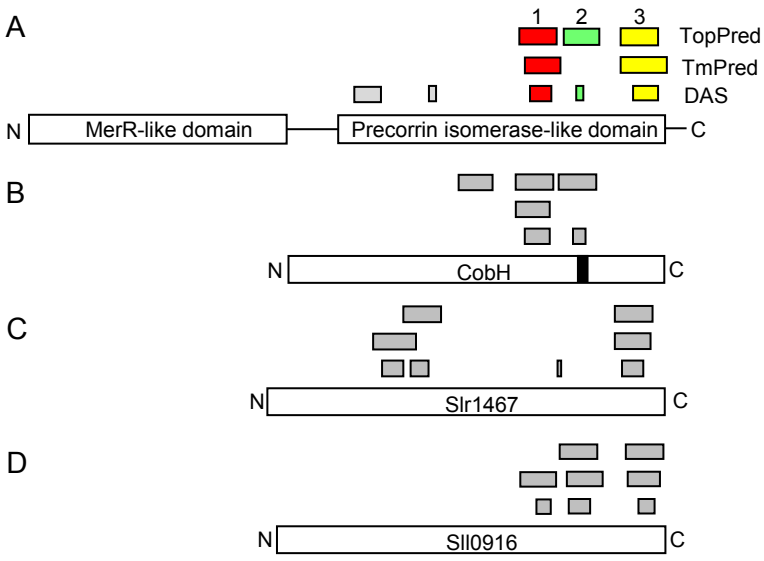

E

Algorithm	Hydrophobic region
DAS	184-198 (15) 226-229 (4) 283-294 (12) 309-312 (4) 341-354 (14)
TMpred	280-299 (20) 334-359 (26)
TopPred	277-297 (21) 302-322 (21) 334-354 (21)

F

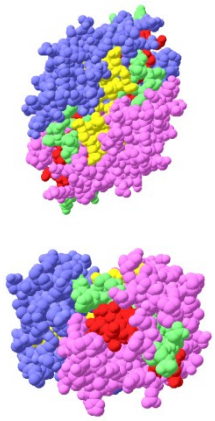

Fig. S1. Analysis of the hydrophobic regions of CoaR. (A) The positions of hydrophobic regions in CoaR are shown as boxed regions (to scale), predicted by the algorithms DAS, TMPred and TopPred. Three predicted hydrophobic regions are apparent towards the carboxyl terminus of the precorrin isomerase-like domain and are colour coded red, green and yellow respectively (a single algorithm, DAS, also detects hydrophobic areas at the N-terminal end of this domain). Regions one and two in CoaR are conserved in the soluble precorrin isomerase homologue from *P. dentrificans,* CobH (B). In CobH, a short hydrophobic loop (shown in black), found in a region analogous to CoaR hydrophobic region two, contributes to dimerisation via hydrophobic packing.[2] Notably, hydrophobic region three is absent in CobH. Slr1467 (C) and Sll0916 (D) are both annotated as precorrin isomerase homologues in the *Synechocystis* genome. Both have a carboxyl terminal hydrophobic region analogous to hydrophobic region three in CoaR and Slr1467 has been shown to be membrane associated *in vivo*.[3] (E) Table summarising the sequence positions and amino acid lengths (in parenthesis) for each of the hydrophobic regions detected in CoaR. The hydrophobic regions predicted by DAS have profile scores greater than the cut-off of 1.7. For TmPred only the regions with scores greater than 500 (the significance threshold level) are shown (871 and 1470 for region one and three respectively). TopPred predicted three regions which scored higher than than the upper cut-off limit for certain candidate hydrophobic/membrane spanning segments (1.354, 1.171 and 1.304 respectively, upper cut-off limit = 1.0). SOSUI predicted CoaR as being a soluble protein (no transmembrane helices were detected) and TMHMM also detected no transmembrane regions. The algorithms are available at the EXPASY website (http://www.expasy.ch/tools/). (F) Space-fill representation of the modelled dimeric structure of the precorrin isomerase-like domain of CoaR. This structure was created by threading residues 162-358 onto the structure of the CobH co-crystallised with hydrogenobyrinic acid (not shown in this model) from *P.denitrificans* (PDB code: 1i1H).[2] C2 symmetry was applied to create the second sub-unit of the dimer. Hydrophobic regions (from both dimer subunits) predicted by TopPred are highlighted using the colour designations from (A). The remaining regions are highlighted blue and magenta for respective dimer subunits. The upper panel shows an extended, surface exposed region of hydrophobicity on one face of the dimer, formed from regions two and three, which traverses the dimer interface. Rotating the dimer (lower panel) shows this region to be exposed via a cleft on one surface of the dimer. Some segments of regions one and two are also seen to be exposed in this representation.

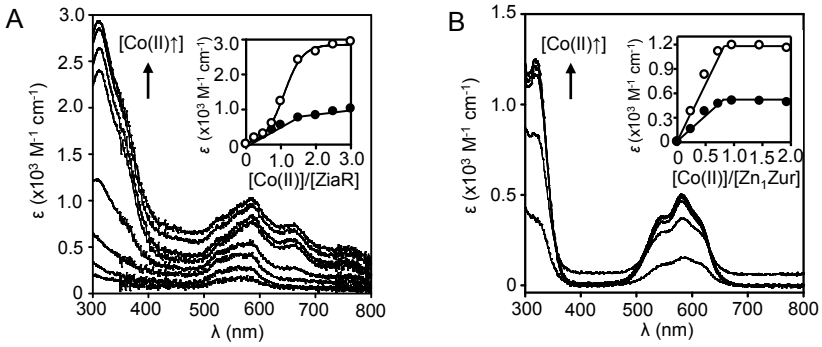

Fig. S2. Co(II) binding to recombinant ZiaR and Zn_1Zur. Apo-subtracted difference spectra following titration of recombinant ZiaR (40 μM) (A) and Zn_1Zur (26 μM) (B) with Co(II). Insets show binding isotherms at 310 nm (open symbols) and 585 nm (closed symbols).

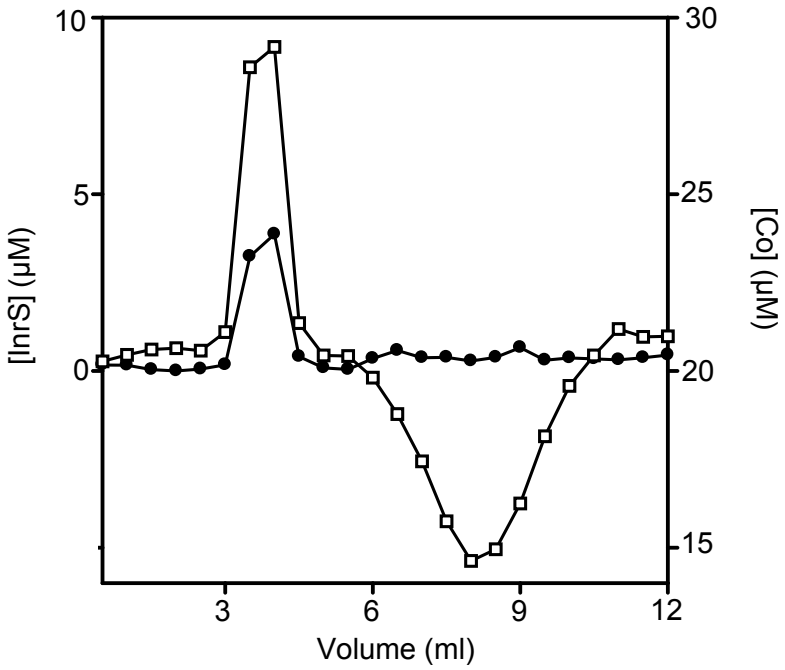

Fig. S3. Resolution of InrS-bound and free Co(II) by gel filtration chromatography. An aliquot (0.5 ml) of InrS (10 μM) (closed symbols) was applied to Sephadex G-25 matrix equilibrated and eluted in buffer containing 400 mM KCl, 100 mM NaCl, 10 mM Hepes (pH 7.8) and 20 μM Co(II). [Co(II)] was determined by ICP-MS (open symbols) and [InrS] determined by calibrated Bradford assay as described previously.[1]

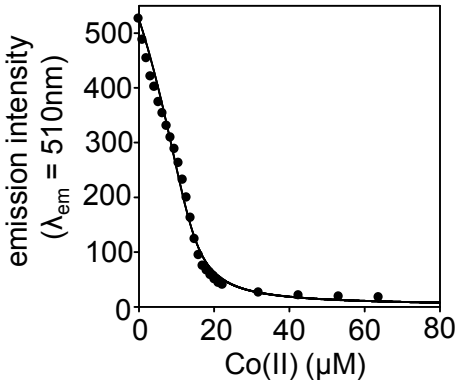

Fig. S4. Determination of Fura-2 $K_{Co(II)}$ by titration with NTA. Fura-2 (4.27 μM) and NTA (10 μM) were titrated with Co(II) in 400 mM KCl, 100 mM NaCl, 10 mM Hepes (pH 7.8) and equilibrium fluorescence intensities recorded (λ_{ex} = 360 nm, λ_{em} = 510 nm). Equilibrium fluorescence emission intensities for each Co(II) addition were fitted by non-linear least squares regression analysis in Dynafit,[4] and $K_{Co(II)}$ for Fura-2 determined. NTA and Fura-2 each bind a single Co(II) atom per chelator molecule and the pH-corrected NTA $K_{Co(II)}$ was determined by the Schwarzenbach's α-coefficient method using equations 2 and 3 below;[1,5, 6]

$$K_A' = K_A\alpha_{H\text{-}L} \qquad (2)$$

$$\alpha_{H\text{-}L} = (1+\beta_{H,1}[H]+\beta_{H,2}[H]^2+\ldots+\beta_{H,n}[H]^n)^{-1} \qquad (3)$$

where K_A' is the pH corrected affinity constant, K_A is absolute affinity constant, $\alpha_{H\text{-}L}$ is Schwarzenbach's α-coefficient, $\beta_{H,1} = 10^{pKa1}$, $\beta_{H,2} = 10^{pKa2}$ etc. and $[H] = 10^{-pH}$. The absolute NTA $K_{Co(II)}$ is 2.4×10^{10} M^{-1}. The sequential acid dissociation constants for NTA are pKa1 = 9.73, pKa2 = 2.49, pKa3 = 1.89.[4] Substituting these values into equation (2) and (3) produces a K_A' Co(II) of 2.78×10^8 M^{-1}($K_{Co(II)} = 3.59 \times 10^{-9}$ M, pH 7.8) for NTA. The $K_{Co(II)}$ for Fura-2 was determined to be 7.03×10^{-9} M ($K_A = 1.42 \times 10^8$ M^{-1}). The fit to the data above assumes some degree of competition with Hepes from the buffer and these data indicate Hepes $K_{Co(II)} = 7.62 \times 10^{-5}$ M).

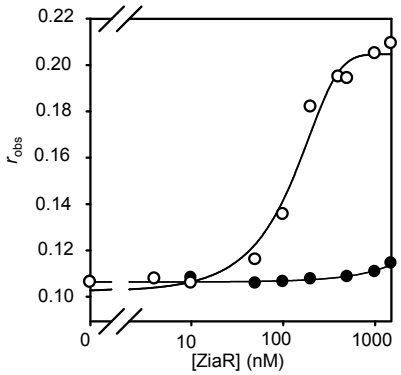

Fig. S5. Effect of Co(II) on association of ZiaR with DNA. Anaerobic titration of *zia*-O/P DNA (10 nM) with recombinant ZiaR in the presence (closed symbols) or absence (open symbols) of 4 μM Co(II) as measured using fluorescence anisotropy.[7]

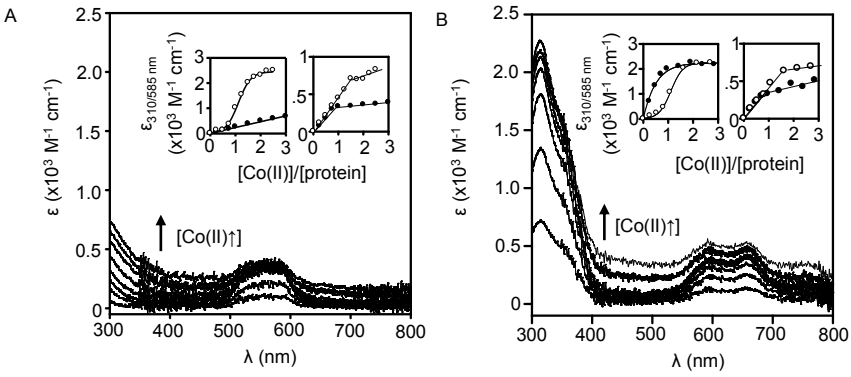

Fig. S6. Co(II) binding to Δα3N ZiaR and Δα5 ZiaR. Apo-subtracted difference spectra collected following anaerobic titration of Δα3N ZiaR (40 μM) (A) and Δα5 ZiaR (42 μM) (B) with Co(II). Insets show binding isotherms monitored at 585 nm (right panels) and 310 nm (left panels) for wild-type ZiaR (open symbols) and Δα3N ZiaR and Δα5 ZiaR (closed symbols). For Δα3N ZiaR, mutation of two predicted metal-binding Cys residues (Cys71, Cys73) resulted in ~50 % reduction in ε_{585nm} at a lower saturating [Co(II)] of ~ one molar equivalent. ε_{310nm} at two molar equivalents is reduced to ~500 M^{-1} cm^{-1} compared to wild-type ZiaR (A). These data are consistent with loss of tetrahedral Co(II) binding at the mutated α3N site (with binding to the α5 site retained) and the involvement of at least one (and likely both) of the mutated Cys residues in Co(II) binding to the α3N site. On titration of Δα5 ZiaR with Co(II), ε_{310nm} increases linearly and Co(II) stoichiometry measured at ε_{310nm} and ε_{585nm} is reduced by ~50 %. Although maximal ε_{310nm} is unchanged, ε_{585nm} is reduced by ~50 % (B). These data are consistent with loss of tetrahedral Co(II) binding to the normally tighter $K_{Co(II)}$ α5 site, with retention of binding to the normally weaker $K_{Co(II)}$ α3N site.

Both Δα3N ZiaR and Δα5 ZiaR retain Zn(II)-responsiveness through the remaining intact metal binding site (Fig. 7). Approximately 0.5 molar equivalents of Zn(II) is required to dissociate Δα3N ZiaR and Δα5 ZiaR *zia*-O/P DNA complexes (Fig. 7) and wild-type ZiaR requires ~ 0.5 molar equivalents of Co(II) for metalloregulation (Fig. 5). These stoichiometry's are lower than previously observed for Zn(II) regulation of wild-type ZiaR,[7] and suggest metalloregulation is possible through a single metal binding site per dimer as is the case for homologous ArsR/SmtB sensors BxmR and CzrA.[8,9] The observation that for wild-type ZiaR the stoichiometry required to dissociate protein-DNA complexes is lower for Co(II) compared to Zn(II) is likely due to α5 $K_{Co(II)}$ being tighter than α3N $K_{Co(II)}$ (Fig. S2); Co(II) preferentially fills the α5 site, occupation of which is sufficient to drive allosteric regulation as observed in figure 5.

```
CoaR            MKTNHLTIKELTDAVGGGVTPRMVRHYHTLGLLPPVQRSEGNYRLYTQQDVQRLQRVIAL 60
CobH            ------------------------------------------------------------

CoaR            KQQGFQLSHIRQLLDSHSEESLDPTLMVQLQQQYQAVIQQITRLRQTASALEGLLGRDQS 120
CobH            ----------------------------------------MPEYDYIRDGNAIYERS 17

CoaR            CQITQAEALAQLKQLDVDVQEGLGKLDQLWTNLDAETTTHPEAFQESLKHLLPDLSAYSE 180
CobH            FAIIRAEA----------------------------------------DLSRFSE 32

CoaR            ITIHLLHQLVLACGDVSLVNAVRLSQGAIASARDALKAGCPVVTDVPVVAAALDQTRLAH 240
CobH            EEADLAVRMVHACGSVEATRQFVFSPDFVSSARAALKAGAPILCDAEMVAHGVTRARLPA 92

CoaR            LGCTVKTLIDDPHITGLREAEQAFWHHDHWQQRLQQIPQGCVLAIGYAPSVLLTACKLIE 300
CobH            GNEVICTLRDP--RTPALAAEIGNTRSAAALKLWSERLAGSVVAIGNAPTALFFLLEMLR 150

CoaR            QQHIQPALVIGMPIGFSHAPGAKRRLMTS--PIPHITIQGSLGGGLLAAVTLNALVETLI 358
CobH            DGAPKPAAILGMPVGFVGAAESKDALAENSYGVPFAIVRGRLGGSAMTAAALNSLARPGL 210

CoaR            AKPDCHCYLTCL 370
CobH            ------------
```

Fig. S7. Multiple sequence alignment between *Synechocystis* CoaR and *P. denitrificans* CobH. Residues known to form hydrogen bonds (directly or indirectly) to HBA in *P. denitrificans* CobH, together with the corresponding CoaR residues, are highlighted in red, CobH residues that are absolutely conserved in CoaR are highlighted on both sequences in green.

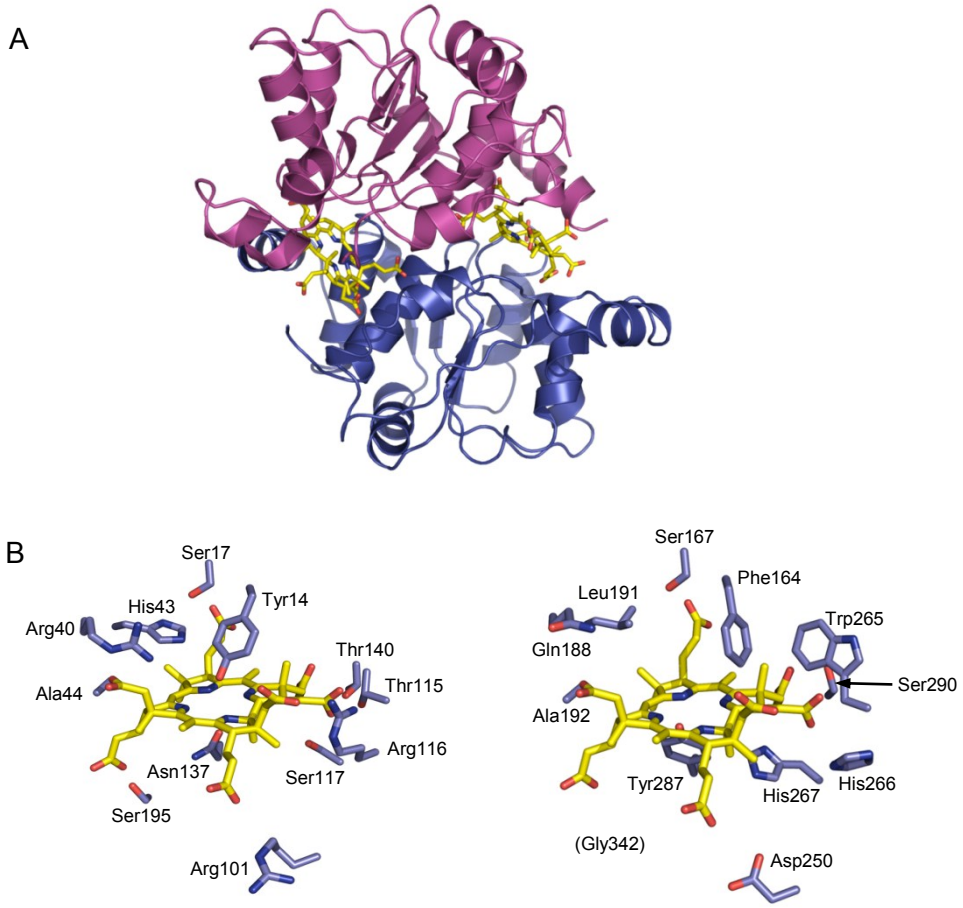

Fig. S8. Comparison of the tetrapyrrole binding sites of CobH and CoaR. (A) Ribbon representation of the modelled structure of the CoaR precorrin isomerase-like domain (from Fig. S1) with the two molecules of hydrogenobyrinic acid from the template CobH co-crystal structure shown as stick models bound at the dimer interface.[2] (B) Simplified view of the tetrapyrrole binding site in CobH and CoaR. Residues known to form hydrogen bonds to hydrogenobyrinic acid in CobH are shown (left panel) in comparison with spatially analogous residues in the modelled CoaR tetrapyrrole binding site (right panel). In CobH Asn137 protrudes into the binding site but does not form part of the hydrogen-bonded complex.[2] CobH Ser195 is in an analogous position to Gly342 in CoaR (side chain H not shown).

Fig. S9. Mathematical descriptions of search time expressions in 2-D and 3-D

For a metal ion diffusing in the cytosol the 3 dimensional search time for binding to a cytosolic protein partner is given by

$$\tau_3 = \frac{L^2}{3D_3} \cdot \frac{L}{b} \quad (4)$$

where L is the radius of the cell, D_3 is the diffusion coefficient of the ion and b is the radius of the target patch (in this case the radius of the protein) that the ion is recognising. A 2 dimensional search, in which the metal ion is restricted to lateral diffusion searching for its protein partner (e.g. in proximity to a negatively charged inner plasma membrane leaflet at which the protein and metal ions are localised), is given by

$$\tau_2 = \frac{L^2}{2D_2} \cdot ln.\frac{L}{b} \quad (5)$$

Assuming $D_2 = D_3$,[10] rearranging equations 4 and 5 produces

$$\frac{\tau_3}{\tau_2} = \frac{2(L/b)}{3ln(L/b)} \quad (6)$$

The complete radius of a *Synechocystis* cell, L, under standard growth conditions has been estimated to be approximately 1.72 μm.[11] The average radius of a protein (from *E.coli*) is approximately 2 nm.[12] Substituting the radii values into equation 6, gives a ratio τ_3/τ_2 of 84.9. Therefore, the search time for an effector ion when searching is restricted to lateral diffusion on the membrane is reduced by almost two-orders of magnitude, which may contribute to co-factor channelling to CoaR but not ZiaR or Zur.

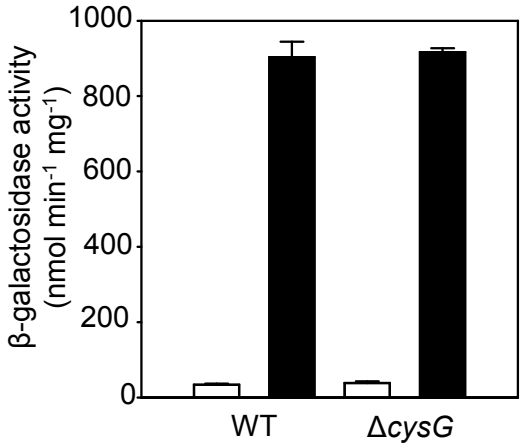

Fig. S10. Co(II)-dependent expression from the *coaT* promoter in wild-type and *ΔcysG E. coli*. The Co(II)-response of the *coaT* promoter was compared in wild-type and *ΔcysG* strains of *E. coli* cultured in the presence (black bars) or absence (white bars) of 100 μM $CoCl_2$ (Mean values from three replicates with standard deviations). No difference in reporter gene expression is evident between wild-type and *ΔcysG E. coli*, indicating that CoaR does not respond to an intermediate synthesised exclusively via the cobaltochelatase activity of CysG.

Supplementary methods

LacZ reporter gene assays in Δ*cysG E. coli*

Reporter gene assays investigating the effect of CysG on Co(II)-dependent expression from the *coaT* promoter were performed in *E. coli* K12 strains obtained from the Coli Genetic Stock Centre (CGSC) (Yale University); the wild type strain (JW331-2) of genotype Δ*(araD-araB)567, ΔlacZ4787(*::*rrnB-3), λ-, rph-1, Δ(rhaD-rhaB)568, hsdR514* was the parental strain for Δ*cysG* mutant strain (BW25113) which contained an additional kanamycin resistance insertion mutation Δ*cysG776*::*kan*. Each strain was transformed with the pET3a*coa* and assays performed as described in the main text for *E. coli* JM101 cells, with cells cultured in the presence/absence of 100 μM $CoCl_2$.

Supplementary References

1. A.W. Foster, C.J. Patterson, R. Pernil, C.R. Hess and N.J. Robinson, Cytosolic Ni(II) sensor in cyanobacterium: nickel detection follows nickel affinity across four families of metal sensors, *J. Biol. Chem*., 2012, **287**, 12142-12151.

2. L.W. Shipman, D. Li, C.A. Roessner, A.I. Scott and J.C. Sacchettini, Crystal structure of precorrin-8x methyl mutase, *Structure*, 2001, **9**, 587-596.

3. A. Mata-Cabana, F.J. Florencio and M. Lindahl, Membrane proteins from the cyanobacterium *Synechocystis* sp. PCC 6803 interacting with thioredoxin, *Proteomics*, 2007, **7**, 3953-3963.

4. P. Kuzmic, Program DYNAFIT for the Analysis of Enzyme Kinetic Data: Application to HIV Proteinase, *Anal. Biochem*., 1996, **237**, 260-273.

5. Z. Xiao and A.G. Wedd, The challenges of determining metal-protein affinities, *Nat. Prod. Rep*., 2010, **27**, 768-789.

6. H. Reyes-Caballero, C.W. Lee and D.P. Giedroc, *Mycobacterium tuberculosis* NmtR harbors a nickel sensing site with parallels to *Escherichia coli* RcnR, *Biochemistry*, 2011, **50**, 7941-7952.

7. S.J. Dainty, C.J. Patterson, K.J. Waldron, and N.J. Robinson, Interaction between cyanobacterial copper chaperone Atx1 and zinc homeostasis, *J. Biol. Inorg. Chem*. 2010, **15**, 77-85.

8. T. Liu, X. Chen, Z. Ma, J. Shokes, L. Hemmingsen, R.A. Scott and D.P. Giedroc, A Cu(I)-sensing ArsR family metal sensor protein with a relaxed metal selectivity profile, *Biochemistry*, 2008, **47**, 10564-10575.

9. S. Lee, A.I. Arunkumar, X. Chen and D.P. Giedroc, Structural insights into homo- and heterotropic allosteric coupling in the zinc sensor *S. aureus* CzrA from covalently fused dimers, *Am. Chem. Soc*., 2006, **128**, 1937-1947.

10. S.E. Halford and J. F. Marko, How do site-specific DNA binding proteins find their targets? *Nucleic Acids Res*., 2004, **32**, 3040-3052.

11. M. Hagemann and E. Zuther, Selection and characterisation of mutants of the cyanobacterium *Synechocystis* sp. PCC 6803 unable to tolerate high salt concentrations, *Arch. Microbiol*., 1992, **158**, 429-434.

12. R. Philips, J. Kondev and J. Theriot, *Physical biology of the cell*, ed. H.G. Garcia, Garland Science, New York, 2009, pp. 26.